Comparison of stabilized finite element methods for simulation of flow of diluted polymeric liquids*

J. Hron[1] and P. Pustějovská[2]

[1]*Mathematical Institute, Charles University in Prague.*
[2]*Institute of Computational Mathematics, Graz University of Technology.*

Abstract

The main aim of this article is the comparison of computational methods for simulations of the flow of polymeric solutions with low concentration and low diffusion. Particularly, we are interested in the simulation of the flow of synovial fluid in the viscous range of deformation which exhibit non-standard viscosity growth. Such response is modeled and discussed in [HMPR10]. First, we focus the description of the numerical discretization of the evolutionary system of governing equations, then we describe the convection dominated problem typical for diluted polymers and introduce three different stabilization methods suitable for the equation of concentration. The results of the used methods are compared on testing problem of driven cavity.

Keywords. Stabilized FEM, SUPG, GLS, CIP, convection-diffusion equation, Péclet number.

1 Introduction

The stabilized finite element method (stabilized FEM) is generally very important tool in computational fluid dynamics, especially for the systems of equations having character close to hyperbolic ones. In our case, as the aim is to model diluted polymeric solutions with low diffusivity, the convective term of the convection-diffusion equation for concentration dominates to diffusion. It is known that standart Galerkin discretization results in a strongly non-stable scheme which then leads to a numerical solution exhibiting non-physical phenomena such as spurious numerical oscillations or sharp layers dislocations.

As to this date there are many stabilization techniques for FEM described in great detail in literature, however we shall not attempt the improvement of the theory of stabilization, instead for our problem we shall use known simple schemes which can be later used in more complicated computations with realistic domains. Moreover, even though there are developed some more sophisticated positiveness preserving methods, we shall focus on the use of methods which preserve the Galrekin or Petrov-Galerkin structure of the problem and are relatively easy to implement, in order not to diverse from the main aim of the application. We shall describe and use for the FEM code following stabilizations: Streamline-upwind Petrov–Galerkin method (SUPG), Galerkin least squares method (GLS) and Continuous interior penalty method (CIP).

The fluid of interest is considered to be incompressible isotropic homogeneous one-constituent fluid. The flow is described by the coupled incompressible generalized Navier–Stokes equations with the convection-diffusion equation. Such a system is suitable as a description of diluted polymeric fluids since the mass concentration of the polymers in the (usually) water fluid background does not reach more than $2-5\%$. Thus, even though a local accumulation of the concentration occurs,

*This work was supported by the project LC06052 (Jindřich Nečas Center for Mathematical Modeling) financed by MŠMT, GAČR grant no. 201/09/0917 and GAUK grant no. 309811/2011.

the density of the fluid as a whole remains almost unchanged. On the other hand, the rheology of the fluid for such local areas of higher concentration can be rapidly diverted from Newtonian behavior, and thus the influence of the concentration on the rheology, in our case on the viscosity, has to be taken into account.

As modeled in the work of [Pus12], we shall consider shear-thinning fluid for which the non-dimensionalized generalized viscosity[1] ν is concentration dependent in a non-standard fashion

$$\nu(c, |\boldsymbol{D}|^2) = \nu_0 \left(\kappa_1 + \kappa_2 |\boldsymbol{D}|^2\right)^{n(c)}. \tag{1.1}$$

Here, c is a scalar concentration of the polymer, $\boldsymbol{D}$ represent the symmetric part of the velocity gradient, κ_1, κ_2 and ν_0 are constants and $n(c)$ is the variable shear-thinning index which shall be specified later.

2 System of equations

Let us introduce the system of non-dimensionalized governing equations, consisting of the constraint of incompressibility, generalized Navier–Stokes equations and convection-diffusion equation for concentration[2]

$$\frac{\partial \boldsymbol{v}}{\partial t} + [\nabla \boldsymbol{v}]\boldsymbol{v} = -\nabla p + \frac{2}{\mathrm{Re}} \operatorname{div}\left(\nu(c, |\boldsymbol{D}|^2)\boldsymbol{D}\right), \tag{2.1}$$

$$\operatorname{div} \boldsymbol{v} = 0, \tag{2.2}$$

$$\frac{\partial c}{\partial t} + (\nabla c) \cdot \boldsymbol{v} = \frac{1}{\mathrm{Pe}} \operatorname{div}\left(D_c(c, |\boldsymbol{D}|^2)\nabla c\right), \tag{2.3}$$

where $\boldsymbol{v}, p, c$ are the unknowns, the velocity vector, and scalar fields of pressure and concentration, respectively. The non-constant viscosity and diffusivity are denoted by ν and D_c. As last, we introduce two characteristic numbers, reduced Reynolds number and Péclet number, characterizing the properties of the flow.

The domain where the system (2.1)–(2.3) is considered, is bounded set in $\mathbb{R}^d$ $(d = 2, 3)$ denoted by Ω with the Lipschitz boundary $\partial\Omega$. We prescribe the Dirichlet and Neumann boundary conditions for both, velocity and concentration. We decompose the boundary on parts Γ^v_{D}, Γ^v_{N} and Γ^c_{D}, Γ^c_{N}, and assume, that $\partial\Omega = \overline{\Gamma^v_{\mathrm{D}} \bigcup \Gamma^v_{\mathrm{N}}}$ and $\Gamma^v_{\mathrm{D}} \bigcap \Gamma^v_{\mathrm{N}} = \emptyset$, similarly for the parts corresponding to concentration. Explicitly, we consider

$$\begin{aligned} (\boldsymbol{v}(t,x)\cdot\boldsymbol{n})\boldsymbol{n} &= \boldsymbol{v}_1(t,x) \quad \text{on } \Gamma^v_{\mathrm{D}}, \\ \boldsymbol{v}_\tau(t,x) &= \boldsymbol{v}_2(t,x) \quad \text{on } \Gamma^v_{\mathrm{D}}, \end{aligned} \qquad c(t,x) = c_D(t,x) \quad \text{on } \Gamma^c_{\mathrm{D}}, \tag{2.4}$$

$$[\boldsymbol{T}(t,x)]\boldsymbol{n} = \boldsymbol{g}^v(t,x) \quad \text{on } \Gamma^v_N, \qquad \boldsymbol{q}_c(t,x)\cdot\boldsymbol{n} = g^c(t,x) \quad \text{on } \Gamma^c_N, \tag{2.5}$$

where $\boldsymbol{n}$ is the unit outward normal to the boundary and $\boldsymbol{v}_\tau = \boldsymbol{v} - (\boldsymbol{v}\cdot\boldsymbol{n})\boldsymbol{n}$. The Neumann boundary conditions for velocity and concentration are prescribed by the Cauchy stress tensor $\boldsymbol{T} = -p\boldsymbol{I} + \frac{2}{\mathrm{Re}}\nu(c, |\boldsymbol{D}|^2)\boldsymbol{D}$ and diffusive flux $\boldsymbol{q}_c = \frac{1}{\mathrm{Pe}} D_c(c, |\boldsymbol{D}|^2)\nabla c$, respectively. These conditions are more physically intuitive because we determine on the boundary physical force density and concentration flux.

The time interval of interest is $I = \langle 0, T\rangle$, for which we have initial conditions $\boldsymbol{v}(0,x) = \boldsymbol{v}_0$ and $c(0,x) = c_0$ for all $x \in \Omega$. We emphasize, that the domain Ω and boundary parts Γ^v_{D}, Γ^v_{N}, Γ^c_{D} and Γ^c_{N} do not change with time.

In what follows, we describe the numerical method suitable for solving this system. First, we discretize the system in time by finite differences method, and then, after obtaining the stationary set of equations for each time step, we use the finite element method for discretizing the space.

[1] From now on for simplicity, we shall call the non-dimensionalized generalized viscosity only by viscosity.

[2] The equation for concentration is in the form without the volumetric production term which corresponds to modeling of synovial fluid. Nevertheless, without any loss of generality, convection-diffusion equation can be extended by the bulk term representing the reactions.

3 Discretization of the system

For the time discretization of the system (2.1)–(2.3) we use θ-scheme, specifically the Crank–Nicholson scheme ($\theta_1 = \theta_2 = 1/2$) see e. g. [DDD70], [TRHG06]. For the incompressibility constraint and the pressure we use the implicit treatment which gives better stability properties and is consistent with the full space-time finite element method discretization. We divide the time interval I into n time steps $\langle t^k, t^{k+1}\rangle$, for $k = 0, ..., n-1$, where $t^0 = 0$ and $t^n = T$, and denote the step length of interval $\langle t^k, t^{k+1}\rangle$ by $\Delta t^k = t^{k+1} - t^k$. Moreover, we approximate the time derivatives by the central differences-like quotient

$$\frac{\partial f}{\partial t} \approx \frac{f(t^{k+1}) - f(t^k)}{\Delta t^k}. \tag{3.1}$$

For simplicity, we assume that Ω has polygonal boundary and thus no boundary approximation is needed. Let us cover the domain by the set $\mathcal{T}_h$ of quadrilaterals denoted by K and define parameter h by

$$h \coloneqq \max_{K \in \mathcal{T}_h} h_K, \tag{3.2}$$

where h_K is, in a suitable sense, a size-measure of the element $K \in \mathcal{T}_h$, the longest size of all elements edges, for example. We require that the mesh fulfills standard regularity conditions, for more detail see [Cia78], which are the local shape regularity and exclusion of hanging nodes. The first one guaranties that with $h \to 0$ the mesh elements shrink uniformly, precisely $h_K/d_K < C$ for all $K \in \mathcal{T}_h$, where d_K is the diameter of the largest ball inscribed into K and C being a constant. The second requirement guaranties that any two elements are either disjoint or have common whole edge or vertex.

For discretization in space, we use standard finite element method, see e. g. [Joh87], [EEHJ96] or [FFS03], based on the discretization of the function spaces to finite dimensional spaces. For our needs, let us define function spaces $\boldsymbol{V}$, P and C as

$$\boldsymbol{V} = \{\boldsymbol{v} \in [W^{1,2}(\Omega)]^d;\ \boldsymbol{v}|_{\Gamma_{\mathrm{D}}^v} = \boldsymbol{0}\}, \tag{3.3}$$

$$P = L^2(\Omega), \tag{3.4}$$

$$C = \{c \in W^{1,2}(\Omega);\ c|_{\Gamma_{\mathrm{D}}^c} = 0\}, \tag{3.5}$$

and the corresponding finite element spaces $\boldsymbol{V}_h$, P_h and C_h

$$\boldsymbol{V}_h = \{\boldsymbol{v} \in [C(\Omega)]^d;\ \boldsymbol{v}|_K \in [Q_2(K)]^d \quad \forall K \in \mathcal{T}_h\}, \tag{3.6}$$

$$P_h = \{p \in L^2(\Omega);\ p|_K \in P_1^{\mathrm{disc}}(K) \quad \forall K \in \mathcal{T}_h\}, \tag{3.7}$$

$$C_h = \{c \in C(\Omega);\ c|_K \in Q_2(K) \quad \forall K \in \mathcal{T}_h\}, \tag{3.8}$$

where $Q_2(K)$ and $Q_1(K)$ denote the space of biquadratic and bilinear functions on the quadrilateral element K, respectively, and $P_1^{\mathrm{disc}}(K)$ denotes the space of linear functions on K, without the requirement of continuity between adjecent elements. All finite element spaces are conforming, since $\boldsymbol{V}_h \subset [W^{1,2}(\Omega)]^d$, $P_h \subset L^2(\Omega)$ and $C_h \subset W^{1,2}(\Omega)$. For the treatment of Dirichlet boundary conditions we also define

$$\boldsymbol{V}_{0h} = \{\boldsymbol{v} \in \boldsymbol{V}_h;\ \boldsymbol{v}|_{\Gamma_{\mathrm{D}}^v} = \boldsymbol{0}\}, \tag{3.9}$$

$$C_{0h} = \{c \in C_h;\ c|_{\Gamma_{\mathrm{D}}^c} = 0\}. \tag{3.10}$$

The combination of velocity and pressure finite element spaces satisfies the Babuška–Brezzi stability condition ([Bab73] or [BF91]) which guaranties the solvability of the coupled discrete system. Our choice (from many) of $Q_2 - P_1^{\mathrm{disc}}$ pair, the biquadratic and discontinuous linear polynomial spaces, is chosen from computational and simplicity reasons. Such combination is known to be stable since, beyond others, the incompressibility constrain is satisfied locally in the weak sense, it means as an "average" on each element of the mesh, see [ESW05].

Now, let us formulate the full discrete system of the equations (2.1)–(2.3) expressed at each discrete time level t^k, $k = 0, ..., n-1$, for the approximations $\boldsymbol{v}_h^{k+1}$, p_h^{k+1} and c_h^{k+1}. Here, the notation of z^k represents $z(t^k)$, and, z_h^k represents the approximation of z^k in corresponding finite element space. To treat the non-homogeneous boundary conditions for velocity and concentration, we assume that there exist functions $\boldsymbol{v}^\star \in [W^{1,2}(\Omega)]^d$ and $c^\star \in W^{1,2}(\Omega)$ such that they satisfy the Dirichlet boundary conditions (2.4) on Γ_{D}^v, Γ_{D}^c, respectively, in sense of traces. Independently of the choice of $\boldsymbol{v}^\star$ and $c^\star$, the approximations of $\boldsymbol{v}^{k+1}$, p^{k+1} and c^{k+1} are $\boldsymbol{v}_h^{k+1}$, p_h^{k+1} and c_h^{k+1}, such that $\boldsymbol{v}_h^{k+1} - \boldsymbol{v}_h^\star \in \boldsymbol{V}_h$, $p_h^{k+1} \in P_h$ and $c_h^{k+1} - c_h^\star \in C_h$, where $\boldsymbol{v}_h^\star \in \boldsymbol{V}_h$ and $\boldsymbol{v}_h^\star|_{\Gamma_D^v} = \boldsymbol{v}_1 + \boldsymbol{v}_2$ and analogously $c_h^\star \in C_h$ and $c_h^\star|_{\Gamma_D^c} = c_D$, satisfying the discrete form of the equations (2.1)–(2.3)

$$
\begin{aligned}
&(\boldsymbol{v}_h^{k+1}, \boldsymbol{\varphi})_\Omega + \theta_1 \Delta t^k \Big(\left([\nabla \boldsymbol{v}_h^{k+1}]\boldsymbol{v}_h^{k+1}, \boldsymbol{\varphi}\right)_\Omega + \frac{2}{\mathrm{Re}} \left(\nu\left(c_h^{k+1}, |\boldsymbol{D}(\boldsymbol{v}_h^{k+1})|^2\right) \boldsymbol{D}(\boldsymbol{v}_h^{k+1}), \nabla \boldsymbol{\varphi}\right)_\Omega \Big) \\
&\qquad - \Delta t^k (p_h^{k+1}, \operatorname{div} \boldsymbol{\varphi})_\Omega - \theta_1 \Delta t^k \left(\boldsymbol{g}^v(t^{k+1}), \boldsymbol{\varphi}\right)_{\Gamma_N^v} \\
&= (\boldsymbol{v}_h^k, \boldsymbol{\varphi})_\Omega - \theta_2 \Delta t^k \Big(\left([\nabla \boldsymbol{v}_h^k]\boldsymbol{v}_h^k, \boldsymbol{\varphi}\right)_\Omega + \frac{2}{\mathrm{Re}} \left(\nu(c_h^k, |\boldsymbol{D}(\boldsymbol{v}_h^k)|^2) \boldsymbol{D}(\boldsymbol{v}_h^k), \nabla \boldsymbol{\varphi}\right)_\Omega \Big) \\
&\qquad + \theta_2 \Delta t^k \left(\boldsymbol{g}^v(t^k), \boldsymbol{\varphi}\right)_{\Gamma_N^v},
\end{aligned}
\tag{3.11}
$$

$$
(\operatorname{div} \boldsymbol{v}_h^{k+1}, \zeta)_\Omega = 0 \tag{3.12}
$$

$$
\begin{aligned}
&(c_h^{k+1}, \psi)_\Omega + \theta_1 \Delta t^k \Big(\left(\nabla c_h^{k+1} \cdot \boldsymbol{v}_h^{k+1}, \psi\right)_\Omega + \frac{1}{\mathrm{Pe}} (D_c(c_h^{k+1}, |\boldsymbol{D}(\boldsymbol{v}_h^{k+1})|^2) \nabla c_h^{k+1}, \nabla \psi)_\Omega \Big) \\
&\qquad - \theta_1 \Delta t^k \left(g^c(t^k), \psi\right)_{\Gamma_N^c} \\
&= (c_h^k, \psi)_\Omega - \theta_2 \Delta t^k \Big(\left(\nabla c_h^k \cdot \boldsymbol{v}_h^k, \psi\right)_\Omega + \frac{1}{\mathrm{Pe}} (D_c(c_h^k, |\boldsymbol{D}(\boldsymbol{v}_h^k)|^2) \nabla c_h^k, \nabla \psi)_\Omega \Big) \\
&\qquad + \theta_2 \Delta t^k \left(g^c(t^k), \psi\right)_{\Gamma_N^c}
\end{aligned}
\tag{3.13}
$$

for all $\boldsymbol{\varphi} \in \boldsymbol{V}_{0h}$, $\zeta \in P_h$, $\psi \in C_{0h}$, and for each time step $k = 1, \ldots, n-1$ with $t^n = T$, where $\boldsymbol{v}^0$ and c^0 are the corresponding initial conditions. Moreover, we assume the fluxes to be functions $\boldsymbol{g}^v \in [L^2(\Gamma_{\mathrm{N}}^v)]^d$, $g^c \in L^2(\Gamma_{\mathrm{N}}^c)$. As standard, we denote the scalar product in $L^2(\Omega)$ by $\int_\Omega fg = (f, g)_\Omega$.

Since the functions spaces $\boldsymbol{V}_h(\boldsymbol{V}_{0h})$, P_h and $C_h(C_{0h})$ have finite dimensions, it is equivalent to satisfy the equations (3.11)–(3.13) only for the bases functions of these spaces. Then, we obtain a finite system of non-linear algebraic equations, written in matrix form as

$$
\begin{aligned}
\left(\mathbf{M}_v + \theta_1 \Delta t^k \mathbf{A}_v(\mathbf{v}^{k+1}, \mathbf{c}^{k+1})\right) \mathbf{v}^{k+1} - \Delta t^k \mathbf{B}^T \mathbf{p}^{k+1} &= \boldsymbol{f}(\mathbf{v}^k, \mathbf{c}^k), \\
\mathbf{B}\mathbf{v}^{k+1} &= 0, \\
\left(\mathbf{M}_c + \theta_1 \Delta t^k \mathbf{A}_c(\mathbf{v}^{k+1})\right) \mathbf{c}^{k+1} &= \boldsymbol{g}(\mathbf{v}^k, \mathbf{c}^k),
\end{aligned}
\tag{3.14}
$$

where $\mathbf{v}^{k+1}$ represents the vector of coefficients obtained by expanding $\boldsymbol{v}_h^{k+1}$ in bases of $\boldsymbol{V}_h$, analogously for $\mathbf{p}^{k+1}$ and $\mathbf{c}^{k+1}$. Next, $\mathbf{M}_v$ and $\mathbf{M}_c$ represent the corresponding mass matrices, $\mathbf{B}$ is the discrete divergence operator, $\mathbf{A}_v(\mathbf{v}, \mathbf{c})$ and $\mathbf{A}_c(\mathbf{v})$ are the operators representing the convection and dissipation/diffusion parts of the corresponding equations and $\boldsymbol{f}$ and $\boldsymbol{g}$ are the non-linear vector functions of vectors from the previous time level. All together, we have $(\dim \boldsymbol{V}_h + \dim P_h + \dim C_h)$ equations, where $(\dim \boldsymbol{V}_h + \dim P_h + \dim C_h) - (\dim \boldsymbol{V}_{0h} + \dim P_h + \dim C_{0h})$ is the number of equations representing the Dirichlet boundary conditions. We need to solve the system of (3.14) for each time step, with initial conditions represented by $\mathbf{v}^0$ and $\mathbf{c}^0$.

If the exact solution is regular enough, the finite element method as we have described above is in space of order of convergence of $p+1$ (p being the polynomial degree of the approximation functions) as $h \to 0$.

4 Computational algorithm

Let us here briefly discuss the algorithm of solution of the algebraic problem (3.14) for one time step. It will be useful to write the algebraic system of equations (3.14) in a more compact way as

$$\boldsymbol{\mathcal{F}}(\mathbf{x}) = 0, \tag{4.1}$$

where $\mathbf{x} = (\mathbf{v}^{k+1}, \mathbf{p}^{k+1}, \mathbf{c}^{k+1})$ is the sought vector at the time step $k+1$, and $\boldsymbol{\mathcal{F}}$ is the non-linear operator representing the discrete system of equations (3.14). In our case, $\boldsymbol{\mathcal{F}}$ is differentiable and has invertible first derivative $\frac{\partial \boldsymbol{\mathcal{F}}}{\partial \mathbf{x}}$ since the Babuška–Brezzi condition is satisfied and all the non-linear terms are continuous in $\mathbf{x}$.

We solve the system (4.1) by using the iterative quasi-Newton method, see for example [Kel95], [Kel03]. For the $n+1$ iteration step it can be formulated as

$$\mathbf{x}^{n+1} = \mathbf{x}^n - \omega^n \left[\frac{\partial \boldsymbol{\mathcal{F}}}{\partial \mathbf{x}}(\mathbf{x}^n)\right]^{-1} \boldsymbol{\mathcal{F}}(\mathbf{x}^n), \tag{4.2}$$

where the parameter $\omega^n \in (0, 1\rangle$ is the damping factor improving the convergence of the Newton method. If the initial guess $\mathbf{x}^0$ is sufficiently close to the solution $\mathbf{x}$, the Newton method gives a quadratic convergence, on the other hand, a poor initial estimate can contribute to its non-convergence. The parameter ω^n is then implemented to ensure the global convergence by adaptively changing the length of the correction vector $\left[\frac{\partial \boldsymbol{\mathcal{F}}}{\partial \mathbf{x}}(\mathbf{x}^n)\right]^{-1} \boldsymbol{\mathcal{F}}(\mathbf{x}^n)$ being sought by standard line search algorithm, for detail see [Deu04].

The block structure of the Jacobian matrix $\frac{\partial \boldsymbol{\mathcal{F}}}{\partial \mathbf{x}}$ is

$$\frac{\partial \boldsymbol{\mathcal{F}}}{\partial \mathbf{x}}(\mathbf{x}) = \begin{pmatrix} \boxtimes & \boxtimes & \boxtimes \\ \boxtimes & 0 & 0 \\ \boxtimes & 0 & \boxtimes \end{pmatrix}, \tag{4.3}$$

where each of its blocks $\boxtimes$ is sparse. This is due to the standard bases selection of the particular finite element spaces. Since we need to compute the derivative $\frac{\partial \boldsymbol{\mathcal{F}}}{\partial \mathbf{x}}$ at each iteration step, it is convenient to approximate the matrix by finite differences from the residual vector $\boldsymbol{\mathcal{F}}(\mathbf{x})$ which is possible because of the matrix sparsity. We write the approximation for $[\frac{\partial \boldsymbol{\mathcal{F}}}{\partial \mathbf{x}}]_{ij}$ which is linearization of i-th equation in j-th unknown

$$\left[\frac{\partial \boldsymbol{\mathcal{F}}}{\partial \mathbf{x}}\right]_{ij}(\mathbf{x}) \approx \frac{[\boldsymbol{\mathcal{F}}]_i(\mathbf{x} + \varepsilon^n \mathbf{e}_j) - [\boldsymbol{\mathcal{F}}]_i(\mathbf{x} - \varepsilon^n \mathbf{e}_j)}{2\varepsilon^n}, \tag{4.4}$$

where $\mathbf{e}_j$ are the unit bases vectors in $\mathbb{R}^m$, with m being the dimension of the vector $\mathbf{x}$, explicitly $m = \dim(\boldsymbol{V}_h \times P_h \times C_h)$, and coefficients ε^n are adaptively taken according to the change in the solution in the previous step.

One iteration of the used method can be summarized in the following steps:

1. Let $\mathbf{x}^n$ be some initial guess.
2. Set the residuum vector $\mathbf{r}^n = \boldsymbol{\mathcal{F}}(\mathbf{x}^n)$ and the Jacobian matrix $\mathbf{A} = \frac{\partial \boldsymbol{\mathcal{F}}}{\partial \mathbf{X}}(\mathbf{x}^n)$.
3. Solve $\mathbf{A}\boldsymbol{\delta} = \mathbf{r}^n$ for the correction $\boldsymbol{\delta}$.
4. Find optimal step length ω^n.
5. Update the solution $\mathbf{x}^{n+1} = \mathbf{x}^n - \omega^n \boldsymbol{\delta}$.

At the step #3 in the quasi-Newton method, the linear problem has to be solved. This can be done either by the direct solver or iterative solver with preconditioning. In our case, of two-dimensional problem, we use sparse direct solver UMFPACK, see for example [Dav04].

5 Convection-dominated problem

The straightforward numerical discretization described above works well for moderate values of Reynolds and Péclet numbers. In the case of diluted polymeric liquids, the Reynolds number is small due to relatively high viscosity. On the other hand, the diffusivity of the polymer in the fluid is extremely small and thus very high Péclet numbers are typical. Due to these reasons, the discretization of equation for velocity behaves as expected, while the algebraic system corresponding to concentration does not meet desired matrix properties and thus the numerical solution exhibits non-physical effects.

Numerical solution of parabolic equation of convection-diffusion with small diffusivity shows spurious oscillations (usually originated at sharp layers) causing the concentration to become locally negative and the sharp layers of the approximate solution are delocalized. This purely numeric feature, worsening with the growing domination of convection, arises from the form of the matrix $\mathbf{A}_c(\mathbf{v})$ associated with the convection and diffusion terms. This phenomena is well known, see for example [Joh82] . For certain combination of velocity, diffusivity and mesh size, the matrix is not diagonally dominant (the absolute value of diagonal matrix entry is smaller than the sum of absolute values of non-diagonal entries), and thus, by most iterative methods the convergence in solving (3.14) is not guaranteed. This relation corresponds to the well known requirement on Péclet number $\mathrm{Pe} \sim D_c^{-1}$ being sufficiently small. There is another thing one should notice, the refinement of the mesh and the choice of the approximation functions of higher order can positively influence the properties of $\mathbf{A}_c(\mathbf{v})$ as well.

We present two-dimensional computations of the evolutionary system (2.1)–(2.3) for two cases. First we consider a test problem with constant viscosity and diffusivity called problem P1, and second, the coupled system describing flow of synovial fluid for which the viscosity has non-standard growth, called problem P2. We specify the reduced Reynolds numbers and the form of non-dimensionalized viscosity, but the Péclet number shall be a subject of variations for the numerical tests, being of the order $10^4 - 10^6$. The lower limit is typical for many polymer solutions, including synovial fluid. Specifically,

$$P1 \begin{cases} \nu = 1, \ \mathrm{Re} = 100, \\ D_c = 1, \ \mathrm{Pe} = \mathrm{const.} \end{cases} \qquad P2 \begin{cases} \nu = \nu_0 \left(\kappa_1 + \kappa_2 |\boldsymbol{D}|^2\right)^{n(c)}, \ \mathrm{Re} = 100, \\ D_c = 1, \ \mathrm{Pe} = \mathrm{const.} \end{cases} \tag{5.1}$$

where

$$n(c) = \omega \left(\frac{1}{\alpha c^2 + 1} - 1 \right). \tag{5.2}$$

The set of equations is considered on $I \times \Omega$, $I = \langle 0, 100 \rangle$ and $\Omega = \langle -1, 1 \rangle \times \langle -1, 1 \rangle$ square. We prescribe the driven cavity-type boundary conditions

$$\Gamma_{\mathrm{D}}: \quad \boldsymbol{v} \cdot \boldsymbol{n} = 0, \qquad c = 0.5, \tag{5.3}$$

$$\boldsymbol{v}_\tau = (x-1)(x+1)\boldsymbol{\tau},$$

$$\Gamma \setminus \Gamma_{\mathrm{D}}: \quad \boldsymbol{v} = \boldsymbol{0}, \qquad \boldsymbol{q}_c \cdot \boldsymbol{n} = 0. \tag{5.4}$$

Using the standard Galerkin finite element method we get the computational results presented in Fig. 9.3 and 9.4 first row, where simulations were computed for three different Péclet numbers. The fashion of the solutions is visible at first sight. With higher Péclet number the Galerkin method produces more spurious oscillations and the values of concentration drops below zero or are higher than the concentration value on boundary Γ_{D}^c. The overshoots and undershoots of concentration are represented by pink/violet color.

It is obvious, that for problems of dominated convection, like in the case of synovial fluid with physical diffusivity of the polymer in the order of $10^{-7}\mathrm{cm}^2/\mathrm{s}$, one has to stabilize the whole system by suitable tools which should eliminate the spurious oscillations but should not significantly change the character of resulting solution. A number of stabilization methods for finite element method has been developed to overcome these typical numerical problems. Today, the most frequently used

stabilization methods are the stream-line diffusion method introduced by Hughes and Brooks in 1979, also called streamline upwind Petrov–Galerkin (SUPG), and the Galerkin least squares (GLS) method. We shall, besides these two, test another alternative, the continuous interior penalty (CIP) method.

Since the discretization of the equation for the velocity and incompressibility constraint are unaltered, let us present and discuss the changes in the discretization of the equation for the concentration, only. We will refer to the equation for concentration before space discretization, thus let us recall it

$$c^{k+1} + \theta_1 \Delta t^k \left(\nabla c^{k+1} \cdot \boldsymbol{v}^{k+1} - \frac{1}{\mathrm{Pe}} \Delta c^{k+1} \right) = c^k - \theta_2 \Delta t^k \left(\nabla c^k \cdot \boldsymbol{v}^k - \frac{1}{\mathrm{Pe}} \Delta c^k \right). \tag{5.5}$$

6 Streamline upwind Petrov–Galerkin method

The SUPG method ([Joh82], [HF89], [FM06]) is motivated by the finite difference method applied on parabolic equation and stabilized by the means of additionally introduced artificial diffusion. In that case, the very small physical diffusivity is increased by suitably chosen τ with the property of $\tau = O(h)$. Even though that the oscillations of the resulting numerical solution are eliminated the added diffusion is introduced in all directions which causes the blurring of sharp layers and non-physical increase of the concentration in some regions.

The SUPG method adds to standard space discretization an additional term "acting" in the streamline direction, treated element-wise,

$$\sum_{K \in \mathcal{T}_h} \tau_K \left(R_{h,K}^{k+1}, \nabla \psi \cdot \boldsymbol{v}_h^{k+1} \right)_K. \tag{6.1}$$

Here, $\{\tau_K\}_{K \in \mathcal{T}_h}$ is a set of stabilization parameters, constants on each element $K \in \mathcal{T}_h$ and $R_{h,K}^{k+1}$ is the residual of equation (5.5) expressed for approximations c_h^{k+1} and c_h^k on each element K[3]

$$R_{h,K}^{k+1} = c_h^{k+1} - c_h^k + \theta_1 \Delta t^k \left(\nabla c_h^{k+1} \cdot \boldsymbol{v}_h^{k+1} - \frac{1}{\mathrm{Pe}} \Delta c_h^{k+1} \right) + \theta_2 \Delta t^k \left(\nabla c_h^k \cdot \boldsymbol{v}_h^k - \frac{1}{\mathrm{Pe}} \Delta c_h^k \right). \tag{6.2}$$

Then, the SUPG method for (5.5) reads for all $\psi \in C_{0h}$

$$\begin{aligned}
&(c_h^{k+1}, \psi)_\Omega + \sum_{K \in \mathcal{T}_h} \tau_K \left(c_h^{k+1}, \nabla \psi \cdot \boldsymbol{v}_h^{k+1} \right)_K \\
&\qquad + \theta_1 \Delta t^k \Big(\left(\nabla c_h^{k+1} \cdot \boldsymbol{v}_h^{k+1}, \psi \right)_\Omega + \frac{1}{\mathrm{Pe}} (\nabla c_h^{k+1}, \nabla \psi)_\Omega \Big) - \theta_1 \Delta t^k \left(g^c(t^{k+1}), \psi \right)_{\Gamma_N^c} \\
&\qquad + \theta_1 \Delta t^k \sum_{K \in \mathcal{T}_h} \tau_K \left((\nabla c_h^{k+1} \cdot \boldsymbol{v}_h^{k+1}, \nabla \psi \cdot \boldsymbol{v}_h^{k+1})_K - \frac{1}{\mathrm{Pe}} (\Delta c_h^{k+1}, \nabla \psi \cdot \boldsymbol{v}_h^{k+1})_K \right) \\
&= (c_h^k, \psi)_\Omega + \sum_{K \in \mathcal{T}_h} \tau_K \left(c_h^k, \nabla \psi \cdot \boldsymbol{v}_h^{k+1} \right)_K \\
&\qquad - \theta_2 \Delta t^k \left[\left(\nabla c_h^k \cdot \boldsymbol{v}_h^k, \psi \right)_\Omega + \frac{1}{\mathrm{Pe}} (\nabla c_h^k, \nabla \psi)_\Omega \right] + \theta_2 \Delta t^k \left(g^c(t^k), \psi \right)_{\Gamma_N^c} \\
&\qquad - \theta_2 \Delta t^k \sum_{K \in \mathcal{T}_h} \tau_K \left((\nabla c_h^k \cdot \boldsymbol{v}_h^k, \nabla \psi \cdot \boldsymbol{v}_h^{k+1})_K - \frac{1}{\mathrm{Pe}} (\Delta c_h^k, \nabla \psi \cdot \boldsymbol{v}_h^{k+1})_K \right)
\end{aligned} \tag{6.3}$$

Recalling that the residual for (in space) exact solution is zero, we obtain

$$\sum_{K \in \mathcal{T}_h} \tau_K \left(R_K^{k+1}, \nabla \psi \cdot \boldsymbol{v}_h^{k+1} \right)_K = 0, \tag{6.4}$$

[3] On each element, the equation in strong form makes sense, since the approximations are the polynomial functions on K.

and thus the SUPG is a consistent method. One can notice that the form of (6.3) can be obtained also by the modification of the test function in the Galerkin scheme as $\psi \longrightarrow \psi + \tau_K \boldsymbol{v} \cdot \nabla \psi$.

What remains is the computation of algorithmic parameter τ_K, which is in fact a crucial question in application of the stabilization method on the convection dominated problem. To this date, there is a notable amount of literature references concerning the τ_K estimation, first time discussed in detail in [BH82]. For the one-dimensional case, the τ_K can be optimally computed which is usually, together with assumptions from the convergence analysis, the base for (non-unique) higher-dimensional extension, [FV00], [Cod00].

From many, we use the proposal of τ_K by [Cod00]

$$\tau_K \sim \left(\frac{c_1}{\mathrm{Pe}\, h_K^2} + \frac{c_2 |\boldsymbol{v}|}{h_K} \right)^{-1}, \tag{6.5}$$

where c_1 and c_2 are constants, coming from the error estimate. However, the constant from inverse inequality can not be, in general, explicitly computed, and thus, the choice of c_1 and c_2 is not obvious. Nevertheless, the values are usually used as in the one-dimensional case, explicitly $c_1 = 4$ and $c_2 = 2$, as has been derived for linear elements, see [Cod00].

For $c^{k+1} \in W^{p+1,2}(\Omega)$ and suitable τ_K (in our case of form (6.5)), the spatial error estimate can be then obtained as

$$||c^{k+1} - c_h^{k+1}||_{SUPG} \leq C \left(\mathrm{Pe}^{-1/2} + h^{1/2} \right) h^p \, |c^{k+1}|_{p+1}, \tag{6.6}$$

where $||\cdot||_{SUPG}$ is a suitable norm, see [RS96]. In comparison with the classical Galerkin formulation, the error has "extra accuracy" of half of power of h in the streamline direction.

7 Galerkin least squares method

While SUPG was motivated by the finite differences method and artificial diffusion, the Galerkin least squares method ([Jia98], [FMM98], [BG09]) is based on formulation of the problem in the sense of minimizing the error functional in a suitable norm, usually the square of L^2-norm, resulting in symmetric positive definite matrix of the algebraic system.

If we set for each time level $k+1$

$$\mathcal{L}_{k+1}(\boldsymbol{v}^{k+1}) c^{k+1} := c^{k+1} + \theta_1 \Delta t^k \left(\nabla c^{k+1} \cdot \boldsymbol{v}^{k+1} - \frac{1}{\mathrm{Pe}} \Delta c^{k+1} \right), \tag{7.1}$$

$$f_k(\boldsymbol{v}^k, c^k) := c^k - \theta_2 \Delta t^k \left(\nabla c^k \cdot \boldsymbol{v}^k - \frac{1}{\mathrm{Pe}} \Delta c^k \right), \tag{7.2}$$

we can formulate the problem (5.5) in the sense of GLS as: find the approximative solution $c_h \in C_h$ such that

$$\|\mathcal{L}_h c_h - f_h\|_2^2 = \min_{\psi \in C_h} \|\mathcal{L}_h \psi - f_h\|_2^2, \tag{7.3}$$

where operator $\mathcal{L}_h = \mathcal{L}_{k+1}(\boldsymbol{v}_h^{k+1})$ and function $f_h = f_k(\boldsymbol{v}_h^k, c_h^k)$.

This can be reformulated as

$$(\mathcal{L}_h c_h - f_h, \mathcal{L}_h \psi)_\Omega = 0 \quad \forall \psi \in C_h, \tag{7.4}$$

or in other words, we are looking for the stationary point for which the derivatives are zero in all directions. The equation (7.4) can be paralleled to standard Galerkin formulation if the test function ψ is replaced by $\mathcal{L}_h \psi$.

At this point, the matrix of the resulting algebraic system is symmetric positive definite. Nevertheless, the operator $\mathcal{L}_h$ is of second order and thus (7.4) is equivalent to solving the $4th$ order equation. Moreover, the formulation requires the direction $\psi \in W^{2,2}(\Omega)$, which is not true

since $C_h \not\subset W^{2,2}(\Omega)$ in the case of the Lagrange finite elements. To resolve this complication, we can choose between two approaches. First, similar to SUPG, one can add to the weak formulation the stabilization term

$$\sum_{K\in\mathcal{T}_h} \tau_K(R_K, \mathcal{L}_h\psi), \tag{7.5}$$

where $R_K = (\mathcal{L}_h c_h - f_h)|_K$ is the residuum on the element K and τ_K is the stabilization parameter. Or, one can reduce the order of the operator $\mathcal{L}_h$ by a suitable reformulation of the equation (5.5). This is an approach we prefer since no additional information about the stabilization parameter is needed.

Let us formally rewrite the (5.5) by the help of additional variable $\boldsymbol{q}$

$$\boldsymbol{q}^{k+1} = \nabla c^{k+1}, \tag{7.6}$$

$$c^{k+1} + \theta_1\Delta t^k \left(\boldsymbol{q}^{k+1}\cdot\boldsymbol{v}^{k+1} - \frac{1}{\mathrm{Pe}}\operatorname{div}\boldsymbol{q}^{k+1}\right) = c^k - \theta_2\Delta t^k\left(\boldsymbol{q}^k\cdot\boldsymbol{v}^k - \frac{1}{\mathrm{Pe}}\operatorname{div}\boldsymbol{q}^k\right). \tag{7.7}$$

Then, in the operator notation defined by

$$\boldsymbol{\mathcal{B}}(\boldsymbol{q}^{k+1}, c^{k+1}) := \boldsymbol{q}^{k+1} - \nabla c^{k+1} \tag{7.8}$$

$$f_k := c^k - \theta_2\Delta t^k(\boldsymbol{q}^k\cdot\boldsymbol{v}^k - \frac{1}{\mathrm{Pe}}\operatorname{div}\boldsymbol{q}^k) \tag{7.9}$$

$$\mathcal{A}(\boldsymbol{q}^{k+1}, c^{k+1}) := c^{k+1} - \theta_1\Delta t^k(\boldsymbol{q}^{k+1}\cdot\boldsymbol{v}^{k+1} - \frac{1}{\mathrm{Pe}}\operatorname{div}\boldsymbol{q}^{k+1}) - f_k \tag{7.10}$$

one gets, after dropping the indexes, the formally reformulated equation (5.5) in the form

$$\mathcal{A}(\boldsymbol{q}, c) = f, \tag{7.11}$$

$$\boldsymbol{\mathcal{B}}(\boldsymbol{q}, c) = \boldsymbol{0}. \tag{7.12}$$

The GLS applied on this system together with boundary conditions represented by operator $\mathcal{C}$ after the space discretization then reads

$$\begin{aligned}&\|\mathcal{A}(\boldsymbol{q}_h, c_h) - f\|_2^2 + \|\boldsymbol{\mathcal{B}}(\boldsymbol{q}_h, c_h)\|_2^2 + \|\mathcal{C}(\boldsymbol{q}_h, c_h)\|_{2,\partial\Omega}^2 \\ &\quad = \min_{\substack{\boldsymbol{w}\in[C_h]^d\\ \psi\in C_h}} \left(\|\mathcal{A}(\boldsymbol{w},\psi) - f\|_2^2 + \|\boldsymbol{\mathcal{B}}(\boldsymbol{w},\psi)\|_2^2 + ||\mathcal{C}(\boldsymbol{w},\psi)||_{2,\partial\Omega}^2\right).\end{aligned} \tag{7.13}$$

This minimum, as the stationary point of (7.13), is then found by solving the system of

$$2\left(\mathcal{A} - f, \frac{\partial\mathcal{A}}{\partial\boldsymbol{q}_h}[\boldsymbol{w}]\right)_\Omega + 2\left(\boldsymbol{\mathcal{B}}, \frac{\partial\boldsymbol{\mathcal{B}}}{\partial\boldsymbol{q}_h}[\boldsymbol{w}]\right)_\Omega + 2\left(\mathcal{C}, \frac{\partial\mathcal{C}}{\partial\boldsymbol{q}_h}[\boldsymbol{w}]\right)_{\partial\Omega} = 0, \tag{7.14}$$

$$2\left(\mathcal{A} - f, \frac{\partial\mathcal{A}}{\partial c_h}[\psi]\right)_\Omega + 2\left(\boldsymbol{\mathcal{B}}, \frac{\partial\boldsymbol{\mathcal{B}}}{\partial c_h}[\psi]\right)_\Omega + 2\left(\mathcal{C}, \frac{\partial\mathcal{C}}{\partial c_h}[\psi]\right)_{\partial\Omega} = 0, \tag{7.15}$$

for all directions $\boldsymbol{w}\in[C_h]^d$ and $\psi\in C_h$. By notation $\frac{\partial\mathcal{A}}{\partial c_h}[\psi]$ is understood the Gâteaux derivative $\frac{\mathrm{d}}{\mathrm{d}\varepsilon}\mathcal{A}(\boldsymbol{q}_h, c_h + \varepsilon\psi)|_{\varepsilon=0}$. The system (7.14) and (7.15) is then the resulting system of non-linear algebraic equations $\boldsymbol{\mathcal{F}}(\mathbf{x}) = 0$.

For the $c\in W^{p+1,2}(\Omega)$ and $\boldsymbol{q}\in[W^{p+1,2}(\Omega)]^d$ one can obtain the error estimate for GLS method

$$||c - c_h||_{1,2} + ||\boldsymbol{q} - \boldsymbol{q}_h||_{1,2} \le Ch^p\left(|c|_{p+1} + |\boldsymbol{q}|_{p+1}\right), \tag{7.16}$$

see [CLMM94], [CLMM97] or [Jia98]. The error estimate of GLS can be however improved for the case of GLS formulation by the means of stabilization term (7.5). Then, one can obtain similar estimate as (6.6), formulated for a GLS suitable norm, see for example [RS96].

8 Continuous interior penalty method

The keystone of continuous interior penalty method ([DD76], [BH04], [BE07], [TO07]) is the penalization of the gradient jumps of the discrete solution on the mesh interfaces, to evoke an apparent stiffness of rapidly changing fields in the space variables (like in the neighborhoods of sharp layers). In contrast to SUPG, the CIP method introduces only one symmetric stabilization term, generally independent of the diffusivity coefficient, which is important for error estimates in the case when diffusivity is non-constant. Then, the mass matrix of resulting algebraical system can be lumped. On the other hand, the CIP method results in more dense matrix of the algebraical system than SUPG or GLS, and from practical point of view, extra information about the interior faces has to be recorded.

Before we formulate the stabilized problem, let us introduce standard notation for discontinuous methods. Let the interior face between two distinct elements K_1 and K_2 of $\mathcal{T}_h$ be called $F = K_1 \cap K_2$, with the diameter h_F and unit outer normal $\boldsymbol{n}$. We call the set of all interior faces of the mesh is called $\mathcal{F}_h$. Then, on each interior face, we define a scalar-valued jump of gradient of scalar field a at the face F between elements K_1 and K_2 as

$$[\nabla a \cdot \boldsymbol{n}]_F = \nabla a|_{K_1} \cdot \boldsymbol{n_1} + \nabla a|_{K_2} \cdot \boldsymbol{n}_2, \tag{8.1}$$

where $\boldsymbol{n}_1$ and $\boldsymbol{n}_2$ are the outer normals with respect to elements K_1 and K_2.

The principle of CIP method is to add to the standard Galerkin discretization the term penalizing the gradient jumps. In the case of discretization scheme by continuous functions, the gradient jump is manifested in the normal direction only, and thus, the form of the penalization is expressed in notation of (8.1) as follows

$$j_1(c_h, \psi) = \sum_{F \in \mathcal{F}_h} \int_F \gamma h_F^2 [\nabla c_h \cdot \boldsymbol{n}]_F [\nabla \psi \cdot \boldsymbol{n}]_F \, \mathrm{d}S \tag{8.2}$$

or in element notation

$$j_1(c_h, \psi) = \sum_{K \in \mathcal{T}_h} \frac{1}{2} \int_{\partial K} \gamma h_{\partial K}^2 [\nabla c_h \cdot \boldsymbol{n}][\nabla \psi \cdot \boldsymbol{n}] \, \mathrm{d}S \tag{8.3}$$

where $[\cdot] = 0$ on $\partial K \cap \partial\Omega$, $h_{\partial K}^2 = h_{F_i}^2$, F_i being the edges of element K, and γ is a user-specified constant. Another possible variant includes the weighting of the stabilization term by the normal flux through each edge, see for example [BF09],

$$j_2(c_h, \psi) = \sum_{K \in \mathcal{T}_h} \frac{1}{2} \int_{\partial K} \gamma h_{\partial K}^2 |\boldsymbol{v}_h \cdot \boldsymbol{n}| [\nabla c_h \cdot \boldsymbol{n}][\nabla \psi \cdot \boldsymbol{n}] \, \mathrm{d}S. \tag{8.4}$$

The CIP stabilization method then reads for each time step $k+1$: find $c_h^{k+1} - c_h^\star \in C_h$ such that[4]

$$\begin{aligned}(c_h^{k+1}, \psi)_\Omega + \theta_1 \Delta t^k \left(\nabla c_h^{k+1} \cdot \boldsymbol{v}_h^{k+1}, \psi\right)_\Omega + \theta_1 \Delta t^k \frac{1}{\mathrm{Pe}} (\nabla c_h^{k+1}, \nabla \psi)_\Omega - \theta_1 \Delta t^k \left(g^c(t^{k+1}), \psi\right)_{\Gamma_N^c} \\ + j(c_h, \psi) = (c_h^k, \psi)_\Omega - \theta_2 \Delta t^k \left(\nabla c_h^k \cdot \boldsymbol{v}_h^k, \psi\right)_\Omega - \theta_2 \Delta t^k \frac{1}{\mathrm{Pe}} (\nabla c_h^k, \nabla \psi)_\Omega + \theta_2 \Delta t^k \left(g^c(t^k), \psi\right)_{\Gamma_N^c} \\ \forall \psi \in C_{0h}. \end{aligned} \tag{8.5}$$

Assuming the exact solution c belongs to $W^{2,2}(\Omega)$[5], the formulation (8.5) is consistent as

$$j(c, \psi) = 0 \qquad \forall \psi \in C_{0h}. \tag{8.6}$$

[4] The treatment of Dirichlet boundary condition is the same as above, thus for the definition of $c_h^\star$ see section 3.

[5] In that case the trace of gradient is well defined.

Moreover, assuming the diffusivity is bounded from zero (the diffusive term does not vanish) and $c^{k+1} \in W^{p+1,2}(\Omega)$, then the a priori error estimate yields

$$||c^{k+1} - c_h^{k+1}||_2 \leq Ch^{p+1}|c^{k+1}|_{p+1}, \tag{8.7}$$

see for example [DD76] or [BH04].

Depending on the choice of penalization (8.3) or (8.4), we abbreviate to CIP1 or CIP2.

9 Comparison of the stabilization methods

Let us recall once again, we resolve the velocity field together with the concentration distribution at the same time. Nevertheless, for the problem P1 the velocity is not influenced by the concentration distribution since for this case, the equations are not fully coupled. For the problem P2 the system of equations is fully coupled and the unstabilized problem diverges on the given mesh.

For comparison of all three stabilization methods, together with the scheme without stabilization for the problem P1, we present Tables 9.2 and 9.1, and the concentration profile cuts in Figure 9.2. All the computations are performed for $\mathrm{Pe} = 10^6$ by the same direct solver.

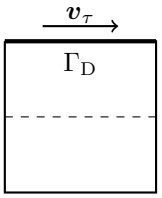

Figure 9.1: Placement of the domain cut, dashed line, at which the concentration profiles are plotted.

Table 9.2 presents the maximal and minimal values of numerical solutions for both computational settings, P1 and P2. Since the analytical solution of concentration must satisfy the principle of maximum/minimum, the interior values of the solution should not exceed its prescribed boundary values, explicitly, in our computational setting, the values $c_{\min} = 0$ and $c_{\max} = 0.5$. We can see, none of the introduced stabilization conserves positiveness. Even though the CIP1 stabilization gives higher over/under–shooting critical values in comparison with SUPG and GLS, they are all concentrated near the boundary, which suggests that the implementation of boundary conditions might need some special treatment for this method. The comparison is performed for the setting of $\mathrm{Pe} = 10^6$.

Method	DOF	#NZ
No stabilization	16,641	263,169
SUPG*	25,091	263,169
GLS	25,091	263,169
CIP1/2	16,641	1.034,289

Table 9.1: The number of degrees of freedom (DOF) for Q_2 approximation of the concentration, the information of sparsity of the matrix of the resulting algebraic system represented by the number of its non-zero entries (#NZ); SUPG* - streamline upwind Petrov–Galerkin, GLS - Galerkin least squares, CIP1/2 - continuous interior penalty (both variants).

The comparison of number of degrees of freedom presents Table 9.1. Since CIP stabilization introduces extra non-zero entries in the resulting approximation system, we present the sparsity of the matrix as well. As we can see, the number of degrees of freedom for basic, non-stabilized, numerical discretization for the mesh of 4096 elements is 16,641, and only the SUPG and GLS

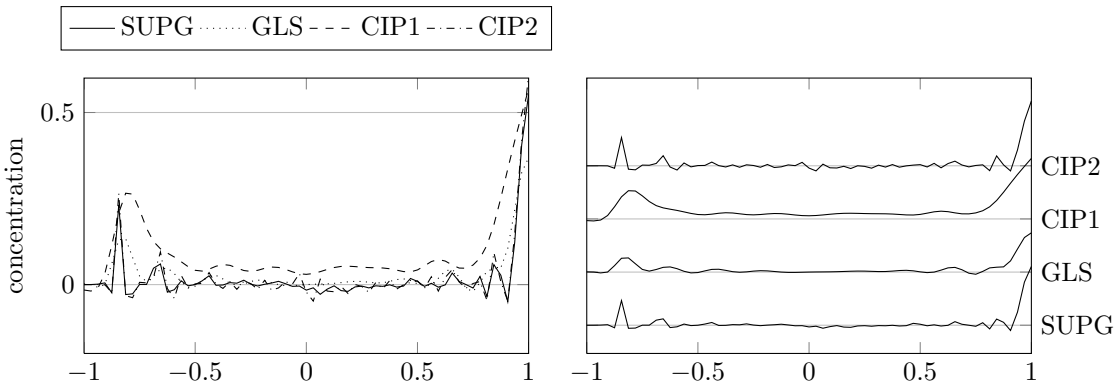

(a) uncoupled test problem P1, Pe = 10^6

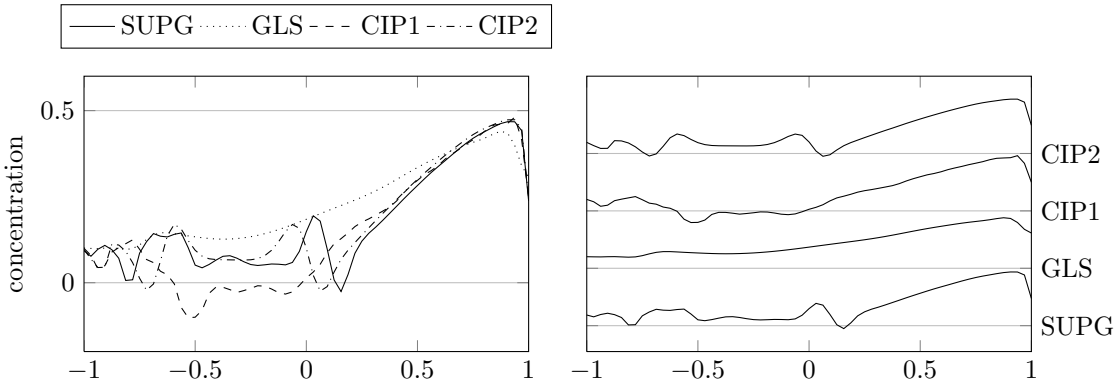

(b) fully coupled problem P2 for synovial fluid, Pe = 10^6

Figure 9.2: Concentration profiles computed by standard and stabilized FEM; profiles on horizontal middle domain cut (see Fig. 9.1) for the test problem P1 (figure (a)) and full problem (figure (b)); gridlines represent the analytical bounds of concentration - $c_{\min} = 0$ and $c_{\max} = 0.5$.

methods increase it. In the case of GLS, that is caused by the additional gradient discretization, in fact we solve the equation of the fourth order, instead of second order. On the other hand, the way we discretize the SUPG is not optimal. For the computation of residuum (6.2) we approximate the gradients as well, resulting in more robust approximation scheme. This might be avoided by, for example, the gradient recovery techniques. For this reason we call streamline upwind Petrov–Galerkin by SUPG* in the Table 9.1, since, generally, the number of degrees of freedom does not need to be increased.

The concentration profiles on one specific domain cut of our computational test domain (see dashed line in Fig. 9.1) are depicted in Figure 9.2. From there and Tab. 9.2 it is clear that CIP1 scheme and GLS are the most diffusive. This is connected with the observations that the concentration values on the specific cuts do not become negative but, on the other hand, the localized concentrations spiral layers are not well preserved. The sharp layers are conserved mostly by GLS method. While SUPG and CIP2 methods are most oscillatory from all the considered stabilizations, for our computations they are least diffusive. From practical point of view, the CIP2, SUPG and GLS methods give similar results. For the SUPG method it is rather crucial to choose suitable stabilizing parameter, for example (6.5). While the CIP2 and GLS methods are almost parameter free, they might need some special treatment for certain boundary conditions.

	P1		P2	
Method	Absolute Min	Absolute Max	Absolute Min	Absolute Max
No stabilization	−0.404	0.737	–	–
SUPG	−0.214	0.568	−0.054	0.507
GLS	−0.165	0.514	−0.021	0.5
CIP1	−0.726	0.624	−0.356	0.856
CIP2	−0.144	0.609	−0.066	0.865

Table 9.2: Comparison of considered stabilization methods concerning the overshoots and undershoots of numerical solution for both computational problems - test problem P1 and fully coupled problem P2 ; SUPG - streamline upwind Petrov–Galerkin, GLS - Galerkin least squares, CIP1/2 - continuous interior penalty (both variants); the analytical bounds of concentration are 0 and 0.5. For both cases Pe = 10^6.

References

[Bab73] I. Babuška. The finite element method with Lagrangian multipliers. *Numerische Mathematik*, 20(3):179–192, 1973.

[BE07] E Burman and Alexandre Ern. Continuous interior penalty hp-finite element methods for advection and advection-diffusion equations. *Mathematics of computation*, 76(259):1119–1140, 2007.

[BF91] F Brezzi and M Fortin. *Mixed and hybrid finite element methods*. Springer-Verlag, New York, 1991.

[BF09] E Burman and M.Á. Fernández. Finite element methods with symmetric stabilization for the transient convection–diffusion–reaction equation. *Computer Methods in Applied Mechanics and Engineering*, 198(33-36):2508–2519, July 2009.

[BG09] PB Bochev and MD Gunzburger. *Least-squares finite element methods*, volume 166. Springer Verlag, New York, 2009.

[BH82] AN Brooks and TJR Hughes. Streamline upwind/Petrov-Galerkin formulations for convection dominated flows with particular emphasis on the incompressible Navier-Stokes equations. *Computer Methods in Applied Mechanics and*, 32(1-3):199–259, 1982.

[BH04] E Burman and P Hansbo. Edge stabilization for Galerkin approximations of convection-diffusion-reaction problems. *Computer methods in applied mechanics and*, 193(15-16):1437–1453, April 2004.

[Cia78] PG Ciarlet. *The finite element method for elliptic problems*. North-Holland, Amsterdam, 1978.

[CLMM94] Z Cai, R Lazarov, TA Manteuffel, and SF McCormick. First-order system least squares for second-order partial differential equations: Part I. *SIAM Journal on Numerical Analysis*, 31(6):1785–1799, 1994.

[CLMM97] Z. Cai, R. Lazarov, T.A. Manteuffel, and S.F. McCormick. First-order system least squares for second-order partial differential equations: Part II. *SIAM Journal on Numerical Analysis*, 34(2):425–454, 1997.

[Cod00] R Codina. On stabilized finite element methods for linear systems of convection-diffusion-reaction equations. *Computer Methods in Applied Mechanics and Engineering*, 188(1-3):61–82, July 2000.

[Dav04] TA Davis. UMFPACK-an unsymmetric-pattern multifrontal method with a column pre-ordering strategy. *ACM Trans. Math. Software*, 30:196–199, 2004.

[DD76] Jim Douglas and Todd Dupont. Interior penalty procedures for elliptic and parabolic Galerkin methods. *Lecture Notes in Physics, Computing methods in applied sciences*, 58(x):207–216, 1976.

[DDD70] J. Douglas Jr, Todd Dupont, and Jim Douglas. Galerkin methods for parabolic equations. *SIAM Journal on Numerical Analysis*, 7(4):575–626, 1970.

[Deu04] P. Deuflhard. *Newton methods for nonlinear problems: affine invariance and adaptive algorithms*, volume 35. Springer Verlag, 2004.

[EEHJ96] K Eriksson, D Estep, P Hansbo, and C Johnson. *Computational differential equations*. Cambridge University Press, 1996.

[ESW05] HC Elman, DJ Silvester, and AJ Wathen. *Finite elements and fast iterative solvers: with applications in incompressible fluid dynamics*. Oxford University Press, USA, 2005.

[FFS03] M Feistauer, J Felcman, and I Straškraba. *Mathematical and Computational Methods for Compressible Flow (Numerical Mathematics and Scientific Computation)*. Oxford University Press, 2003.

[FM06] T Fries and H Matthies. A stabilized and coupled meshfree/meshbased method for the incompressible Navier–Stokes equations—Part II: Coupling. *Computer Methods in Applied Mechanics and Engineering*, 195(44-47):6191–6204, September 2006.

[FMM98] JM Fiard, TA Manteuffel, and SF McCormick. First-order system least squares (FOSLS) for convection-diffusion problems: Numerical results. *SIAM Journal on Scientific Computing*, 19(6):1958–1979, 1998.

[FV00] LP Franca and F. Valentin. On an improved unusual stabilized finite element method for the advective-reactive-diffusive equation. *Computer Methods in Applied Mechanics and Engineering*, 190(13):1785–1800, December 2000.

[HF89] TJR Hughes and LP Franca. A new finite element formulation for computational fluid dynamics: VIII. The galerkin/least-squares method for advective-diffusive equations. *Computer Methods in Applied*, 73(604912):173–189, 1989.

[HMPR10] J Hron, J Málek, P Pustějovská, and K.R. Rajagopal. On the Modeling of the Synovial Fluid. *Advances in Tribology*, 2010(Art. No. 104957), 2010.

[Jia98] Bo-nan Jiang. *The Least-squares finite element method*. Springer, 1998.

[Joh82] C Johnson. *Finite element methods for convection-diffusion problems*. North-Holland, Amsterdam, 1982.

[Joh87] C. Johnson. *Numerical solution of partial differential equations by the finite element method*, volume 32. Cambridge University Press, Studentlitteratur, Lund, February 1987.

[Kel95] C.T. Kelley. *Iterative methods for linear and nonlinear equations*. Society for Industrial Mathematics, Philadelphia, 1995.

[Kel03] C.T. Kelley. *Solving nonlinear equations with Newton's method*, volume 1. Society for Industrial Mathematics, Philadelphia, 2003.

[Pus12] P Pustějovská. *Biochemical and mechanical processes in synovial fluid – modeling, analysis and computational simulations.* Phd thesis, Charles University in Prague, 2012.

[RS96] HG Roos and M Stynes. *Numerical methods for singularly perturbed differential equations*, volume 24. Springer Verlag, Berlin, 1996.

[TO07] S Turek and A Ouazzi. Unified edge-oriented stabilization of nonconforming FEM for incompressible flow problems: Numerical investigations. *Journal of Numerical Mathematics*, 15(4):299–322, 2007.

[TRHG06] S Turek, L Rivkind, J Hron, and R Glowinski. Numerical Study of a Modified Time-Stepping θ-Scheme for Incompressible Flow Simulations. *Journal of Scientific Computing*, 28(2-3):533–547, March 2006.

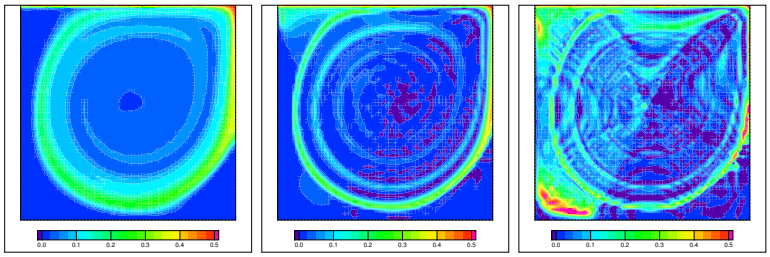

(a) none, $\mathrm{Pe} = 10^4$ (b) none, $\mathrm{Pe} = 10^5$ (c) none, $\mathrm{Pe} = 10^6$

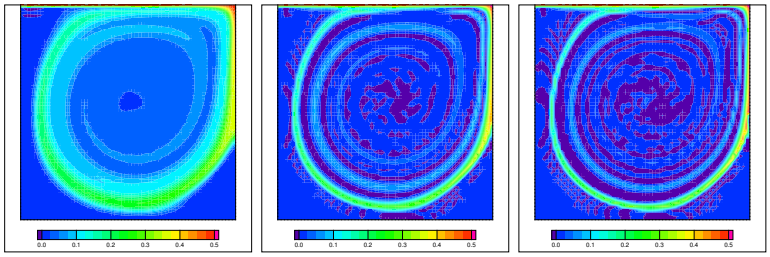

(d) SUPG, $\mathrm{Pe} = 10^4$ (e) SUPG, $\mathrm{Pe} = 10^5$ (f) SUPG, $\mathrm{Pe} = 10^6$

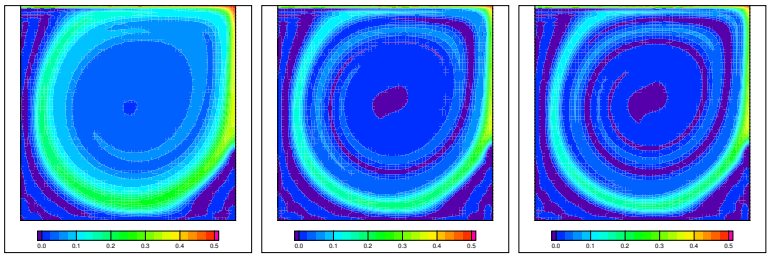

(g) GLS, $\mathrm{Pe} = 10^4$ (h) GLS, $\mathrm{Pe} = 10^5$ (i) GLS, $\mathrm{Pe} = 10^6$

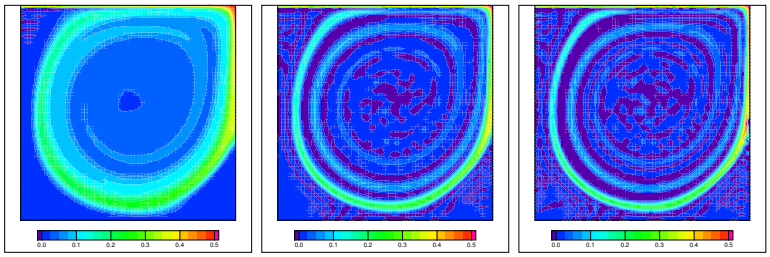

(j) CIP1, $\mathrm{Pe} = 10^4$ (k) CIP1, $\mathrm{Pe} = 10^5$ (l) CIP1, $\mathrm{Pe} = 10^6$

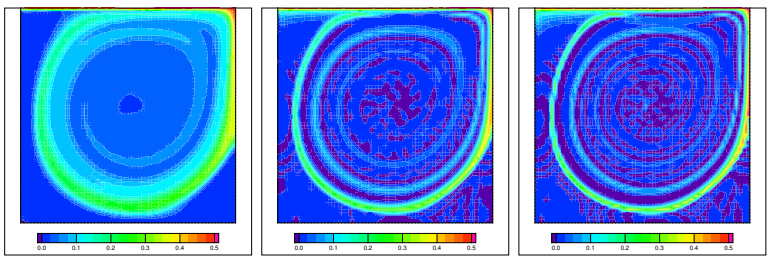

(m) CIP2, $\mathrm{Pe} = 10^4$ (n) CIP2, $\mathrm{Pe} = 10^5$ (o) CIP2, $\mathrm{Pe} = 10^6$

Figure 9.3: Computational results of concentration distribution for boundary conditions (5.4) for test problem P1; in comparison classical and different stabilized FEM; plotted at time $t = 50$.

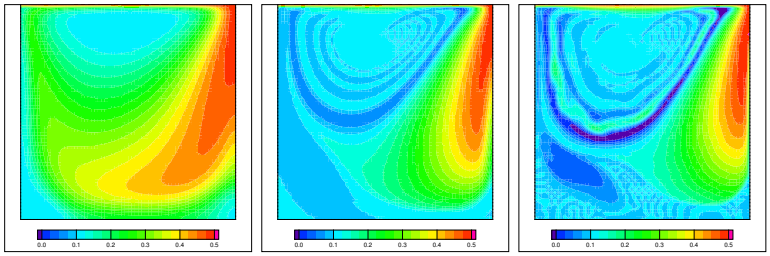

(a) SUPG, $\mathrm{Pe} = 10^4$ (b) SUPG, $\mathrm{Pe} = 10^5$ (c) SUPG, $\mathrm{Pe} = 10^6$

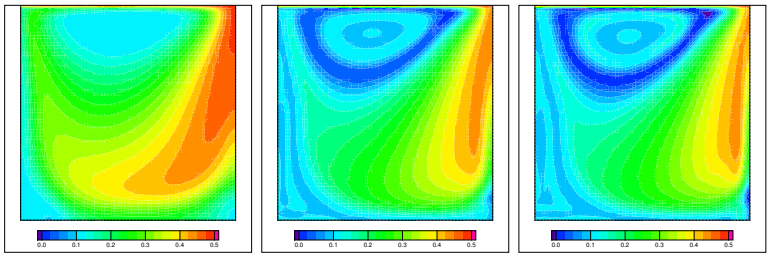

(d) GLS, $\mathrm{Pe} = 10^4$ (e) GLS, $\mathrm{Pe} = 10^5$ (f) GLS, $\mathrm{Pe} = 10^6$

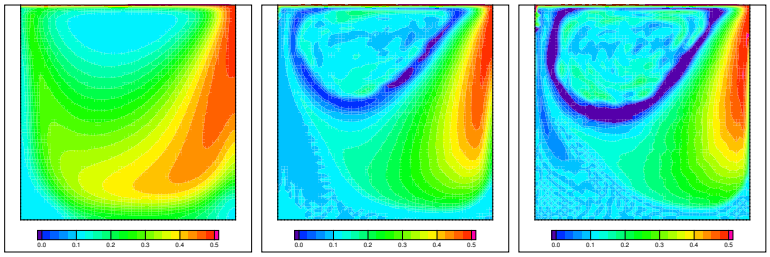

(g) CIP1, $\mathrm{Pe} = 10^4$ (h) CIP1, $\mathrm{Pe} = 10^5$ (i) CIP1, $\mathrm{Pe} = 10^6$

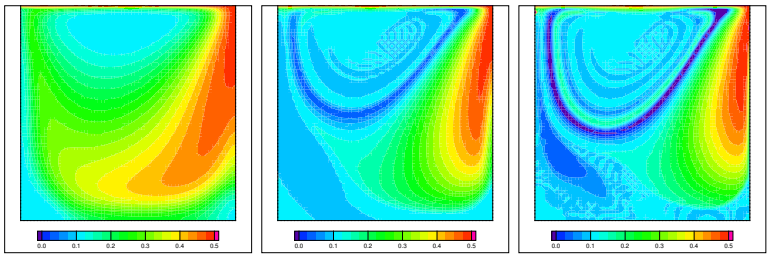

(j) CIP2, $\mathrm{Pe} = 10^4$ (k) CIP2, $\mathrm{Pe} = 10^5$ (l) CIP2, $\mathrm{Pe} = 10^6$

Figure 9.4: Computational results of concentration distribution for boundary conditions (5.4) for fully coupled problem P2; in comparison classical and different stabilized FEM; plotted at time $t = 150$. Results without stabilizations are not available due to non-convergence.